nature geoscience

SUPPLEMENTARY INFORMATION

https://doi.org/10.1038/s41561-018-0214-5

In the format provided by the authors and unedited.

A distinct metal fingerprint in arc volcanic emissions

Marie Edmonds[1]*, Tamsin A. Mather[2] and Emma J. Liu[1]

[1]Department of Earth Sciences, University of Cambridge, Cambridge, UK. [2]Department of Earth Sciences, University of Oxford, Oxford, UK.
*e-mail: marie.edmonds@esc.cam.ac.uk

Supplementary Material

A distinct metal fingerprint in arc volcanic emissions

M. Edmonds, T. A. Mather, E. J. Liu

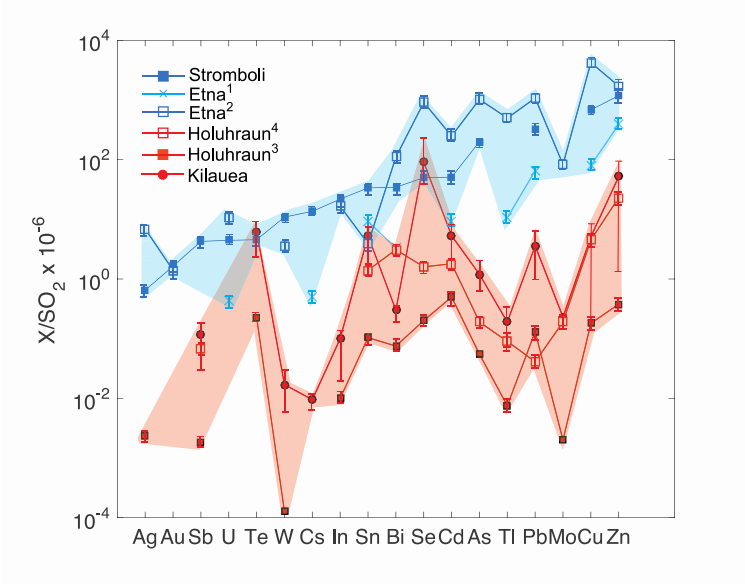

Supplementary figure 1: Ratios X/SO_2, in mg/kg, in the gas plumes volcanoes from arc (blue) and ocean island settings (red). Volcanoes are Stromboli (solid blue squares), Etna (light blue crosses[1] and blue open squares[2]), Kīlauea (red circles) and Holuhraun, Iceland (red squares[3] and open squares[4]). Elements are ordered using the Stromboli dataset, as **Figure 1** of the main paper. See **table 1** for citations and errors on data.

Contribution of metals to the volcanic plume as silicate ash particles

Volcanic particulates sampled by filter packs in plumes are made up of both aerosols (aqueous liquids with dissolved acid gases into which metals partition from high temperature magmatic vapor, before being condensed upon quenching in the atmosphere) and also silicate particles, fragments of bubble walls typically launched into the plume by bubble bursting. The bulk analysis of the particulate fraction then inevitably results in some of the metal budget being sourced from the silicate particles rather than metals that have been volatilized from the magma forming the aerosol and gas phases. This effect is most significant for the less mobile, more lithophile elements, and less important for the more volatile metals, with high vapor-melt partition coefficients. Here we discuss the magnitude of this effect.

At Stromboli a minor silicate contribution was inferred for Cr, Cs, Cu, Rb and W (0-5%), but a significant one for Te and Zn (10%) and corrected accordingly[3]. For Etna, it has been noted that significant concentrations of Al, Si, Na, K, and REE are present in the plume, which must be sourced from silicate material[2]. Elements such as Se, Cd and Sb, however, which are present only in trace amounts in silicate melts, are present in significant quantities in filter pack analyses (greater than more abundant lithophile trace elements such as Th, Sc), suggesting that these metals are volatile. The weight ash fraction (WAF) was calculated by these authors[2] using the abundance of REE. The calculated WAF is very low for Bi (0.1%), Sb (0.2%), Se and Tl (both 0.1%); slightly more significant for Pb (3%), As (2%) and Cu (6%) but significant for Mo, Zn, Te and W (33, 25, 59, 100% respectively), although Te is poorly constrained by its low abundance (close to detection, table 1) in lavas. There is abundant evidence from elsewhere that Te is highly volatile[4]. Another study used Th abundance to calculate the proportion contributed from ash and derived considerably lower estimates: zero for Tl, Bi, Cd; then 3% for Cu, 1% for Sn, 2% for Zn and 0.5% for Pb[1]. At Ambrym negligible ash contributions were inferred for Ag, Au, Sn, Bi, Se, Cd, As, Tl, with a slightly larger contribution for Cs (0-15%), Pb (~2%), Cu (0-17%) and Zn (7-40%)[5]. For Holuhraun the concentrations of Th and REE were used to estimate very low proportion of silicate ash (about 10 µg of ash per filter on average) and therefore the effect of ash contamination was neglected[6]. An ash correction was not calculated for the Kīlauea dataset.

Solid sulfides, oxides, halides, and oxyhydroxides might also be present in the plume, given the dramatic fall in solubility of gaseous metal chloride, sulfide and other species during the drop in temperature from the basalt liquidus temperature to ambient conditions. The presence of these phases may impact the estimation of silicate ash fraction because even nominally "immobile" high field strength elements like Sn, Th or REE may have significant volatility in the presence of abundant gaseous F, as is well known from studies of greisen-forming ore-bearing hydrothermal systems e.g.[7].

We conclude that while in some cases up to 40% of a metal or semi-metal species might be supplied from ash, in general the metals we plot here are highly volatile and their abundance is controlled dominantly by transport initially in the magmatic vapor phase and later (at and away from the vent) in liquid aerosol.

Metal-carrying capacity of magmatic vapor phase at low pressures

Experimental studies[8] and thermodynamic modeling have shown that metals form stable complexes with chloride, sulfate and fluoride in volcanic plumes[9]. Volcanic gas at the surface is the low density phase which is the result of separation of a brine phase from a saline supercritical fluid as it decompresses and cools (**supplementary figure 2**). Up to now, much of the literature on metals in volcanic environments has been gleaned from condensates[10,11], deposited during shallow cooling of magmatic fluids, which have little relevance to the question of how mafic volcanic systems outgas metals to the atmosphere[12]. Little data exists for hot magmatic plumes outgassed directly from the magma column during eruptions, which are expected to contain a far higher load of metals dispersed into the atmosphere, either as gas or as sub micron-aerosols, owing to their higher temperature and chloride content[13,14].

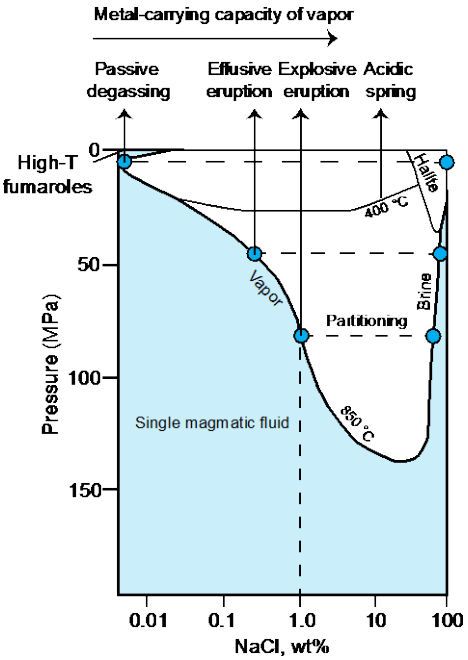

Supplementary figure 2: NaCl-H_2O phase diagram plotted in pressure-composition space, modified after[15].

The solvus will shrink significantly at high temperatures, increasing the salinity and metal-carrying capacity of outgassing vapor. It is possible that supercritical metal-rich fluids may reach the surface, avoiding immiscibility. Until recently[16,17], it was assumed by some authors that low salinity volcanic gas would not have the capacity to dissolve large quantities of metals as chloride complexes, and the brine phase was therefore the favored ore-forming medium[18]. **Figure 1 (main paper)** shows that, on the contrary, volcanic gases are highly significant carriers of metals.

Table 1, below, shows the data used in this paper and its sources. We focus here on active basaltic volcanoes with data acquired using filter packs at the vent (*i.e.* not from fumaroles or lava flows, or as condensates and sublimates).

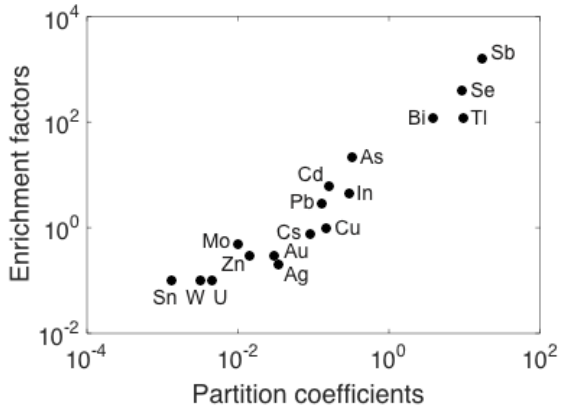

Supplementary Figure 3: Enrichment factors from **table 1** for elements in the plume of Etna (Italy), using Cu as a normalising element, plotted against “absolute” partition coefficients (defined as mass of element in the gas/mass of element in the melt phase) calculated by estimating a dilution factor for the plume[12].

Table 1: Metal/semi-metals contents of degassed lavas and gas/aerosol samples; X/SO_2, metal fluxes, volatilities and enrichment factors for the datasets presented in the main paper.

Erupted lava metal content, in ppm. Data sources: Stromboli Volcano (Italy)[3], Holuhraun (Iceland)[6], Etna (Italy)[2], Ambrym Volcano (Vanuatu)[5], Kīlauea (Hawaii, USA), standard BHVO[19] and Masaya Volcano (Nicaragua)[20]. Error typically <10% for ICP-MS, IMA with internal calibration using standards.

Gas and aerosol metal data, in $\mu g/m^3$, from Stromboli Volcano (Italy)[3], Holuhraun (Iceland)[6], Etna (Italy)[1], Ambrym Volcano (Vanuatu)[5], Kīlauea Volcano (Hawaii, USA)[14] and Masaya Volcano (Nicaragua)[20]. Uncertainties are shown in brackets for each element within each dataset and are typically 5-25%.

Flux of element *X* in kg per day, calculated using the mass ratio X/SO_2* and the independently measured flux of SO_2 (data sources as above). The uncertainty on the flux measurement is 30-32%, propagated from errors on SO_2 flux (~30%) and errors on gas and aerosol measurements (5-10%).

* X/SO_2, in mg/kg; errors on X/SO_2 are propagated from errors on analysis of S and X in gas/aerosol phase and including, where available[21], the standard deviation of repeat analyses on the same day, amounting to 7-17% for the former and up to 95% for the latter[21].

Emanation coefficient, ε_x, is calculated as the percentage of the metal *x* that has degassed from the silicate melt, equal to: $\varepsilon_x = (c_i - c_f) / c_i$,

where c_i is the initial concentration of element x in the magma and c_f is the final concentration of element *x* in the post-eruptive lava (as originally defined by[22]. The *emanation coefficients* given are estimated in a range of ways (which are indicated as footnotes for each sub-table). The *emanation coefficient* ε_x of these elements from the magma can be assessed from their mean enrichment factor (EF) and the emanation coefficient of Pb from molten basalt (which may be assumed to be constant at 0.01[23]), as[1,3,24]: $\varepsilon_x^{-1} = 1 + \left[\left(EF_{Pb} / EF_x \right) \left(1 - \varepsilon_{Pb} \right) / \varepsilon_{Pb} \right]$. We also calculate the concentration of metals and semi-metals in the silicate melt prior to degassing, c_i. The amount of metal (or semi-metal) in the gas plume was "added" back into to the degassed lava composition by converting the mass X/SO_2 ratio in the plume and then multiplying by the pre-eruptive melt concentration of sulfur (from melt inclusion concentrations, corrected for matrix glass sulfur concentration[5 6 25,26]). This amount, in ppm, was added to the degassed lava composition to estimate a "un-degassed" magma composition c_i. For some datasets we also calculate emanation coefficients using *X/Cl* to estimate pre-degassing metal concentrations in the melt, using melt inclusion and matrix glass concentrations as shown in the footnotes. Errors on the *emanation coefficients* are propagated from typical errors on the individual electron microprobe analyses of sulfur, which is typically 5%, and errors on X/SO_2. Total errors therefore range from 9 to 13%. However, when uncertainty related to the sulfur and chlorine outgassing budget are taken into account, errors may exceed 20% (these are shown in **figure 2** of the main paper), particularly for *emanation coefficients* calculated using plume *X/Cl*.

EF_{Cu} is the *enrichment factor* relative to copper (Cu), equal to $EF_{Cu} = \frac{\left(\frac{[X]}{[Cu]}\right)_{gas}}{\left(\frac{[X]}{[Cu]}\right)_{lava}}$. Errors are propagated from the individual metal analyses and range from 14-17%.

Note on propagation of errors: X/SO_2, enrichment factors and emanation coefficients are calculated using the measured concentration data as defined above, with individual errors as defined in the paper sources (see tables below). Errors on these quantities are propagated from the error on the individual measurements, where the uncertainty on quantity z (which is a function of independent variables x and y e.g. z = xy, or z = x/y) is the sum of the squares of the fractional errors, or error percentages, of x and y: $\frac{\delta z}{z}\sqrt{\left(\frac{\delta x}{x}\right)^2+\left(\frac{\delta y}{y}\right)^2}$.

Volcano	**Stromboli**[3]								
Elements	*Lava, ppm*	*Gas, aerosol, μg/m³*	*Flux, kg/day*	*X/SO₂, mg/kg*	*X/Cl, mg/kg*	*Emanation coefficient ε (%)*[a]	*Emanation coefficient ε (%)*[b]	*Emanation coefficient ε (%)*[c]	EF_{Cu}
S	40	4540 (±227)	4.15×10^5 ($\pm 1.26 \times 10^5$)			98	99	98	
Cl	550	2910 (±146)	1.40×10^5 ($\pm 4.25 \times 10^4$)			74	79	71	
Ag	0.51	6.0×10^{-3} (±0.0003)	0.27 (±0.08)	0.65 (±0.05)	2.06 (±0.22)	0.14	0.82	0.54	0.3 (±0.045)
Au	0.07	2.0×10^{-3} ($\pm 2.0 \times 10^{-4}$)	0.68 (±0.22)	1.64 (±0.18)	0.69 (±0.08)	1.5	13	1.3	0.8 (±0.14)
Sb	0.25	3.3×10^{-2} ($\pm 3.3 \times 10^{-3}$)	1.77 (±0.56)	4.27 (±0.48)	11.3 (±1.2)	4	10	5.8	3.8 (±0.65)
U	4.0	2.4×10^{-2} ($\pm 1.2 \times 10^{-3}$)	1.85 (±0.56)	4.45 (±0.31)	8.25 (±0.90)	0.06	0.72	0.28	0.2 (±0.03)
Te	0.7	2.0×10^{-2} ($\pm 1.0 \times 10^{-3}$)	1.89 (±0.57)	4.55 (±0.32)	6.87 (±0.76)	0.52	4.1	1.3	0.8 (±0.12)
W	2.5	1.0×10^{-1} ($\pm 1.0 \times 10^{-2}$)	4.53 (±1.43)	10.9 (±1.22)	34.4 (±3.8)	0.52	2.8	1.8	1.2 (±0.21)
Cs	3.8	1.8×10^{-1} ($\pm 1.8 \times 10^{-2}$)	5.66 (±1.79)	13.6 (±1.52)	61.9 (±6.8)	0.44	2.3	2.2	1.4 (±0.24)
Sn	0.70	1.1×10^{-1} ($\pm 5.5 \times 10^{-3}$)	14.0 (±4.26)	33.6 (±2.38)	37.8 (±4.2)	2.0	24	6.8	4.6 (±0.69)
Bi	0.14	1.7×10^{-1} ($\pm 8.5 \times 10^{-3}$)	14.3 (±4.35)	34.5 (±2.44)	58.4 (±6.4)	11	62	36	35.2 (±5.3)
Se	0.05	7.4×10^{-1} ($\pm 7.4 \times 10^{-2}$)	20.8 (±6.58)	50.0 (±5.59)	254 (±28)	41	87	87	429 (±74)
Cd	0.07	4.8×10^{-1} ($\pm 2.4 \times 10^{-2}$)	21.1 (±6.42)	50.9 (±3.60)	165 (±18)	17	83	76	199 (±30)
As	4.30	3.0 (±0.3)	83.0 (±26.3)	200 (±22.4)	1030 (±110)	5	23	24	20.2 (±3.5)
Tl									
Pb	16.2	1.3 (±0.065)	132 (±40.2)	318 (±22.5)	447 (±49)	1	11	3.6	2.3 (±0.35)
Mo									
Cu	87	3.0 (±0.15)	283 (±86.1)	682 (±48.2)	1030 (±110)	0.39	4.8	1.6	1.0 (±0.15)
Zn	112	0.40 (±0.04)	491 (±155)	1180 (±132)	137 (±15)	0.83	6.4	0.17	0.1 (±0.017)

[a] *Emanation coefficient* calculated assuming $\varepsilon_{Pb} \sim 1\%$[22,23] (see table caption), from[3].
[b] *Emanation coefficient* calculated using plume *X/SO₂* and the mass of sulfur degassed (from matrix and melt inclusion glass analysis; see table caption and methods). Melt inclusion and matrix glass data from[3,27] (0.34 and 0.004 wt% sulfur).
[c] *Emanation coefficient* calculated using plume *X/Cl* and the mass of chlorine degassed (from matrix and melt inclusion glass analysis; see table caption and methods). Melt inclusion and matrix glass data from[3,27] (0.19 and 0.055 wt% chlorine).

Volcano	**Holuhraun[6]**						
Elements	*Lava ppm*	*Gas, aerosol[a] μg/m³*	*Flux, kg/day*	*X/SO₂ mg/kg*	*Emanation coefficient ε (%)[b]*	*Emanation coefficient ε (%)[c]*	*EF_{Cu}*
S	400[28]	185 (±19)				74	500 (±85)
Cl		3.64 (±0.36)		1.97×10^4 ($\pm 2.2 \times 10^3$)		32	42 (±7.1)
Ag	0.28	1.54×10^{-3} ($\pm 1.5 \times 10^{-4}$)	0.23 (±0.04)	2.41×10^{-3} ($\pm 2.7 \times 10^{-4}$)	1.8×10^{-3}	1.9×10^{-3}	5.9 (±1.0)
Au							
Sb	0.026	2.47×10^{-3} ($\pm 2.5 \times 10^{-4}$)	0.18 (±0.06)	1.82×10^{-3} ($\pm 2.0 \times 10^{-4}$)	1.5×10^{-2}	1.5×10^{-2}	103 (±18)
U							
Te	0.0048	1.58×10^{-1} ($\pm 1.6 \times 10^{-2}$)	22.3 (±7.1)	2.28×10^{-1} ($\pm 2.5 \times 10^{-2}$)	9.2	9.5	35800 (±6200)
W	0.093	7.30×10^{-5} ($\pm 7.3 \times 10^{-6}$)	1.2×10^{-2} ($\pm 3.8 \times 10^{-3}$)	1.26×10^{-4} ($\pm 1.0 \times 10^{-5}$)	2.9×10^{-4}	3.0×10^{-4}	0.9 (±0.16)
Cs							
Sn	0.99	7.28×10^{-2} ($\pm 7.3 \times 10^{-3}$)	10.2 (±3.2)	1.04×10^{-1} ($\pm 1.1 \times 10^{-2}$)	2.2×10^{-2}	2.2×10^{-2}	80.0 (±14)
Bi	0.025	4.80×10^{-2} ($\pm 4.8 \times 10^{-3}$)	7.28 (±2.3)	7.5×10^{-2} ($\pm 8.4 \times 10^{-3}$)	6.4×10^{-1}	6.6×10^{-1}	2080 (±360)
Se	0.014	1.68×10^{-1} ($\pm 1.7 \times 10^{-2}$)	19.6 (±6.2)	2.01×10^{-1} ($\pm 2.2 \times 10^{-2}$)	2.9	3.1	12800 (±2200)
Cd	0.23	3.30×10^{-1} ($\pm 3.3 \times 10^{-2}$)	48.7 (±15.4)	4.99×10^{-1} ($\pm 5.6 \times 10^{-2}$)	4.5×10^{-1}	4.8×10^{-1}	1540 (±270)
As	0.27	4.09×10^{-2} ($\pm 4.1 \times 10^{-3}$)	5.38 (±1.7)	5.50×10^{-2} ($\pm 6.2 \times 10^{-3}$)	4.4×10^{-2}	4.5×10^{-2}	167 (±30)
Tl	0.01	6.07×10^{-3} ($\pm 6.1 \times 10^{-4}$)	0.73 (±0.23)	7.46×10^{-3} ($\pm 8.3 \times 10^{-4}$)	1.6×10^{-1}	1.6×10^{-1}	658 (±114)
Pb	0.51	8.79×10^{-2} ($\pm 8.8 \times 10^{-3}$)	12.8 (±4.1)	1.31×10^{-1} ($\pm 1.5 \times 10^{-2}$)	5.4×10^{-2}	5.7×10^{-2}	186 (±32)
Mo	0.40	1.26×10^{-3} ($\pm 1.3 \times 10^{-4}$)	0.2 (±0.06)	2.01×10^{-3} ($\pm 2.2 \times 10^{-4}$)	1.1×10^{-3}	1.1×10^{-3}	3.4 (±0.6)
Cu	142	1.30×10^{-1} ($\pm 1.3 \times 10^{-2}$)	17.7 (±5.6)	1.80×10^{-1} ($\pm 2.0 \times 10^{-2}$)	2.7×10^{-4}	2.8×10^{-4}	1.0 (±0.2)
Zn	100	2.37×10^{-1} ($\pm 2.4 \times 10^{-2}$)	36.9 (±11.7)	3.79×10^{-1} ($\pm 4.2 \times 10^{-2}$)	8.0×10^{-4}	8.3×10^{-4}	2.6 (±0.5)

[a] sample name BAR-A from[6]

[b] *Emanation coefficient* (expressed in terms of a %) from[6], calculated using a dilution factor (calculated using at-vent and downwind plume sulfur dioxide concentrations). Error propagated from gas measurements are in the range 10-20%.

[c] *Emanation coefficient* calculated assuming the degassing of 1100 ppm sulfur, from 1500 ppm to 400 ppm[28] and using the X/SO_2 ratio of the plume to reconstruct the concentration of element X prior to degassing.

Volcano	**Etna**[2]							
	Lava	*Gas, aerosol*[a]	*Flux,*	*X/SO$_2$*[e]*,*	*Emanation coefficient*	*Emanation coefficient*	*Emanation coefficient*	*EF$_{Cu}$*
	ppm	*μg/m^3*	*kg/day*	*mg/kg*	*ε (%)*[b]	*ε (%)*[c]	*ε (%)*[d]	
Elements:								
S	150	181 (±19)	5.0×10^6 ($\pm 1.7 \times 10^6$)					71 (±9)
Cl	1700	67 (±7)	9.2×10^5 ($\pm 3.0 \times 10^5$)	1.85×10^5 ($\pm 2.0 \times 10^4$)	39.9	56.4	0.80	2.3 (±0.3)
Ag	0.9	2.5×10^{-3} ($\pm 2.5 \times 10^{-4}$)	35 (±12)	6.91 (±0.77)	4.47	8.36	0.07	0.2 (±0.035)
Au	0.1	5.1×10^{-4} ($\pm 5.1 \times 10^{-5}$)	7.0 (±2.3)	1.41 (±0.16)	7.91	14.3	0.10	0.3 (±0.05)
Sb	0.12	3.32 (±0.33)	4.5×10^4 (±1.5)	9.17×10^3 ($\pm 1.0 \times 10^3$)	99.8	99.9	85	1630 (±282)
U	2.5	3.8×10^{-3} ($\pm 3.8 \times 10^{-4}$)	52.5 (±17.3)	10.5 (±1.2)	2.50	4.75	0.035	0.1 (±0.012)
Te								
W	1	1.3×10^{-3} ($\pm 1.3 \times 10^{-4}$)	18.0 (±5.94)	3.59 (±0.4)	2.14	4.09	0.035	0.1 (±0.017)
Cs	0.8	0.01 (±0.001)	138 (±46)	27.6 (±3.1)	17.4	29.1	0.26	0.74 (±0.13)
Sn	1.5	1.4×10^{-3} ($\pm 1.4 \times 10^{-4}$)	19.3 (±6.8)	3.87 (±0.43)	1.55	2.97	0.035	0.1 (±0.017)
Bi	0.02	4.0×10^{-2} ($\pm 4.0 \times 10^{-3}$)	552 (±182)	110 (±12)	97.1	98.5	29	118 (±20.4)
Se	0.05	3.3×10^{-1} ($\pm 3.3 \times 10^{-2}$)	4560 (±1500)	912 (±101)	99.1	99.5	58	388 (±67.2)
Cd	0.85	9.0×10^{-2} ($\pm 9.0 \times 10^{-3}$)	1243 (±435)	249 (±27)	64.1	77.7	2.1	6.2 (±1.1)
As	1	3.7×10^{-2} ($\pm 3.7 \times 10^{-3}$)	511 (±179)	102 (±11)	38.4	54.9	7.12	22 (±3.8)
Tl	0.09	1.8×10^{-1} ($\pm 1.8 \times 10^{-2}$)	2486 (±870)	497 (±55)	97.1	98.5	29	118 (±20.4)
Pb	8	3.9×10^{-1} ($\pm 3.9 \times 10^{-2}$)	5387 (±1890)	1077 (±120)	45.1	61.5	1.0	2.9 (±0.50)
Mo	3.7	3.0×10^{-2} ($\pm 3.0 \times 10^{-3}$)	414 (±145)	82.9 (±9.2)	12.0	21.0	0.17	0.5 (±0.09)
Cu	90	1.53 (±0.15)	2.11×10^4 ($\pm 7.4 \times 10^3$)	4227 (±470)	22.3	35.8	0.35	1.0 (±0.17)
Zn	110	6.2×10^{-1} (±0.062)	8564 (±3000)	1710 (±1.90)	8.67	15.6	0.10	0.3 (±0.05)

[a] ET1 of[2]

[b] *Emanation coefficient* calculated using plume *X/SO$_2$* and the mass of sulfur degassed (from matrix and melt inclusion glass analysis; see table caption and methods). Melt inclusion and matrix glass data from (0.32 and 0.015 wt% sulfur)[26].

[c] *Emanation coefficient* calculated using plume *X/Cl* and the mass of chlorine degassed (from matrix and melt inclusion glass analysis; see table caption and methods). Melt inclusion and matrix glass data from (0.28 and 0.17 wt% chlorine)[26].

[d] *Emanation coefficient* calculated assuming $\varepsilon_{Pb} \sim 1\%$[22,23] (see table caption and methods).

[e] Note that these X/SO_2 values are high compared with other arc volcanoes in this dataset and with other data from Etna[1,29], which causes the emanation coefficients to be anomalously high when using the X/SO_2 ratio, combined with the melt inclusion sulfur contents, to reconstruct the metal contents of the melts (main paper, **figure 2**).

Volcano	**Masaya**[20]				
	Lava ppm	*Gas, aerosol, $\mu g/m^3$*	*X/SO_2, mg/kg*	*Flux, kg/day*	*EF_{Cu}*
Elements					
S	150	0.11 (±0.006)	5.0×10^5 [30] ($\pm 6.0 \times 10^4$)	5.0×10^5 ($\pm 1.65 \times 10^4$)	2.8×10^3 ($\pm 0.4 \times 10^3$)
Cl					
Ag					
Au					
Sb	0.321	0.0074 (±0.00074)	0.35 (±0.04)	0.18 (±0.06)	0.92 (±0.12)
U	1.55	0.01 (±0.001)	0.48 (±0.05)	0.24 (±1.2)	0.26 (±0.034)
Te	0.033	0.19 (± 0.019)	9.0 (±1.0)	4.5 (±1.5)	230 (±29)
W					
Cs	0.711	0.029 (±0.0029)	1.38 (±0.15)	0.69 (±0.23)	1.6 (±0.21)
In					
Sn					
Bi	0.023	0.061 (±0.006)	2.90 (±0.32)	1.5 (±0.5)	110 (±14)
Se					
Cd	0.113	0.22 (±0.022)	20.9 (±2.3)	11 (±3.6)	77 (±10)
As					
Tl	0.092	0.21 (±0.021)	20.0 (±2.2)	10 (±3.4)	91 (±12)
Pb	3.36	0.142 (±0.014)	13.5 (±1.5)	6.7 (±2.2)	1.7 (±0.22)
Mo					
Cu	251	6.32 (±0.063)	600 (±67)	300 (±99)	1.0 (±0.33)
Zn	144	1.69 (±0.17)	160 (±18)	80 (±26)	0.47 (±0.06)

Volcano	**Kīlauea**								
	Lava[19]	*Gas, aerosol*[14]	*Flux,*	*X/SO$_2$*	*X/Cl*	*Emanation coefficient*	*Emanation coefficient*	*Emanation coefficient*	*EF$_{Cu}$*
	ppm	*μg/m^3*	*kg/day*	*mg/kg*	*mg/kg*	*ε (%)*[a]	*ε (%)*[b]	*ε (%)*[c]	
Elements:									
S		120 (±13)	7×10^8 [14] ($\pm 65 \times 10^6$)			89	89	44	
Cl	402	16 (±1.5)	448 (±45)	640 (±45)		0.42	30	3.3	
Ag	3.32×10^{-1}								
Au	1.5×10^{-3}								
Sb	1.7×10^{-1}	2.5×10^{-3} ($\pm 0.4 \times 10^{-4}$)	0.07 (±0.06)	0.12 (±0.01)	1.6×10^2 (±20)	0.16	0.22	1.46	13.7 (±2.1)
U	4.2×10^{-1}	3.6×10^{-5} ($\pm 5.0 \times 10^{-6}$)		0.0029 ($\pm 3 \times 10^{-4}$)	2.3 (±0.3)	0.0016	0.16	0.0087	0.080 (±0.02)
Te	6.3×10^{-3}	1.34×10^{-1} ($\pm 1.5 \times 10^{-2}$)	4.8 (±3.0)	6.3 (±0.7)	8.4×10^3 ($\pm 1 \times 10^3$)	70	99	96	1.98×10^4 ($\pm 3.8 \times 10^3$)
W	2.80×10^{-1}	1.46×10^{-4} ($\pm 2.6 \times 10^{-5}$)	1.4×10^{-2} ($\pm 8.0 \times 10^{-3}$)	0.017 ($\pm 2 \times 10^{-3}$)	9.1 (±1.3)	0.014	0.97	0.053	4.86×10^{-1} (±0.11)
Cs	8.6×10^{-2}	1.38×10^{-4} ($\pm 3.0 \times 10^{-5}$)	6.0×10^{-3} ($\pm 2.0 \times 10^{-3}$)	9.5×10^{-3} ($\pm 1 \times 10^{-3}$)	8.6 (±1.3)	0.025	2.92	0.16	1.50 (±0.4)
In	4.6	1.00×10^{-3} ($\pm 1.0 \times 10^{-4}$)	8.0×10^{-2} ($\pm 7.0 \times 10^{-2}$)	0.1 ($\pm 1 \times 10^{-2}$)	63 (±10)	0.0050	0.41	18	202 (±37)
Sn	2.15	5.1×10^{-2} ($\pm 9.0 \times 10^{-3}$)	4.5 (± 2.3)	5.3 ($\pm 6 \times 10^{-1}$)	3.2×10^3 ($\pm 5 \times 10^2$)	0.56	31	2.3	22.1 (±5.2)
Bi	1.5×10^{-1}	4.3×10^{-3} ($\pm 1.9 \times 10^{-4}$)	0.21 (±0.07)	0.3 ($\pm 3 \times 10^{-2}$)	2.7×10^2 (±40)	0.46	35	22	267 (±43)
Se	1.4×10^{-1}	1.49 (±0.15)	62.5 (±45)	91 (±10)	9.3×10^4 ($\pm 1 \times 10^4$)	60	99	99	1.39×10^5 ($\pm 2.5 \times 10^4$)
Cd	1.2×10^{-1}	1.03×10^{-1} ($\pm 1.2 \times 10^{-2}$)	3.8 (±2.3)	5.3 (±0.6)	6.4×10^3 ($\pm 1 \times 10^3$)	9.2	94	46	800 (±150)
As	1.5	2.73×10^{-2} ($\pm 2.0 \times 10^{-3}$)	1.1 (±0.5)	1.2 (±0.1)	1.7×10^3 ($\pm 3 \times 10^3$)	0.18	25.4	1.8	17.0 (±2.9)
Tl	4.9×10^{-2}	2.8×10^{-3} ($\pm 0.4 \times 10^{-3}$)	0.13 (±0.07)	0.19 (±0.02)	1.8×10^2 (±30)	0.88	52	5.5	53.3 (±11)
Pb	4.0	4.0×10^{-2} ($\pm 0.3 \times 10^{-2}$)	3.1 (±2.3)	3.6 (±0.4)	2.5×10^3 (±400)	0.21	16	1	9.32 (±1.6)
Mo	9.50×10^{-1}	4.7×10^{-3} ($\pm 0.5 \times 10^{-3}$)	1.7×10^{-1} (±0.1)	0.23 (±0.03)	2.9×10^2 (±50)	0.056	8.5	0.50	4.61 (±0.86)
Cu	137	1.5×10^{-1} ($\pm 9.0 \times 10^{-3}$)	4.5 (±4.0)	5.1 (±0.06)	9.4×10^3 ($\pm 1.5 \times 10^3$)	0.0086	2.0	0.11	1.00 (±0.16)
Zn	102	1.50 (±0.17)	45 (±44)	52 (±6)	9.4×10^4 ($\pm 1.3 \times 10^4$)	0.12	22	1.5	13.7 (±2.6)

[a] *Emanation coefficient* calculated using plume *X/SO$_2$* and the mass of sulfur degassed (from matrix and melt inclusion glass analysis; see table caption and methods). Melt inclusion and matrix glass data: 0.13 and 0.015 wt% sulfur[31].
[b] *Emanation coefficient* calculated using plume *X/Cl* and the mass of chlorine degassed (from matrix and melt inclusion glass analysis; see table caption and methods). Melt inclusion and matrix glass data: 0.05 and 0.035 wt% chlorine[25]. Note that the uncertainty on this emanation coefficient is high owing to the low concentration of Cl in the plume and the uncertainty associated with estimating the chlorine budget from melt inclusions and matrix glasses[21,32].
[c] *Emanation coefficient* calculated assuming $\varepsilon_{Pb} \sim 1\%$[22,23] (see table caption and methods).

Volcano	**Ambrym**[5]				
	Lava[5], *ppm*	*Gas, aerosol*[5], *μg/m*^{3}	*Flux, kg/day*	*Emanation coefficient ε (%)*[a]	EF_{Cu}
Elements					
S	0.015			95	
Cl	0.07			30	
Ag		3.20 (±0.19)	23 (±4.0)		
Au		3.1×10^{-3} ($\pm 1.9 \times 10^{-4}$)	1.6 (±0.5)		
Sb					
U	0.5	1.3×10^{-2} ($\pm 5.2 \times 10^{-4}$)		0.3	2.1 (±0.33)
Te					
W					
Cs	1.1	1.8×10^{-2} ($\pm 1.1 \times 10^{-3}$)	12 (±3.7)	0.3	1.3 (±0.21)
Sn	1	0.8 (±0.08)	1500 (±470)	18	64.5 (±11.8)
Bi		4.1×10^{-2} ($\pm 1.6 \times 10^{-3}$)	32 (±9.7)	6.2	
Se		3.1×10^{-1} (±0.03)	360 (±114)	5.9	
Cd	0.15	3.2×10^{-2} ($\pm 3.2 \times 10^{-3}$)	46 (±15)	7.4	17.2 (±3.2)
As	1.7	0.25 (±0.025)	300 (±95)	4.1	11.9 (±2.2)
Tl	0.08	0.195 (±0.012)	160 (±49.0)	26	197 (±32.4)
Pb	5.9	0.09 (±0.004)	90 (±27)	0.3	1.2 (±0.19)
Mo					
Cu	129.00	1.60 (±0.10)	1300 (±400)	0.18	1.00 (±0.16)
Zn	89.5	0.58 (±0.035)	350 (±110)	0.11	0.52 (±0.086)

[a] *Emanation coefficient* calculated using measurements of ε_{Pb} from[5] (see table caption and methods).

Comparison of different ways to calculate emanation coefficients

The tables above show various different ways to estimate the emanation coefficient, defined as $\varepsilon_x = (c_i - c_f)/c_i$, where c_i is the initial concentration of element *x* in the magma and c_f is the final concentration of element *x* in the post-eruptive lava (as originally defined by[22]). The plots shown in **supplementary figure 4** show how they compare to one another. The emanation coefficients calculated using the various methods are broadly consistent with one another in terms of order of volatility, with the methods using X/SO_2 and *X/Cl* to "add back" metals in the proportions given by these ratios to calculate c_i and thus emanation coefficient yielding higher emanation coefficients than the methods based on measurement of the emanation coefficient of ^{210}Pb[23], by 1-20 times.

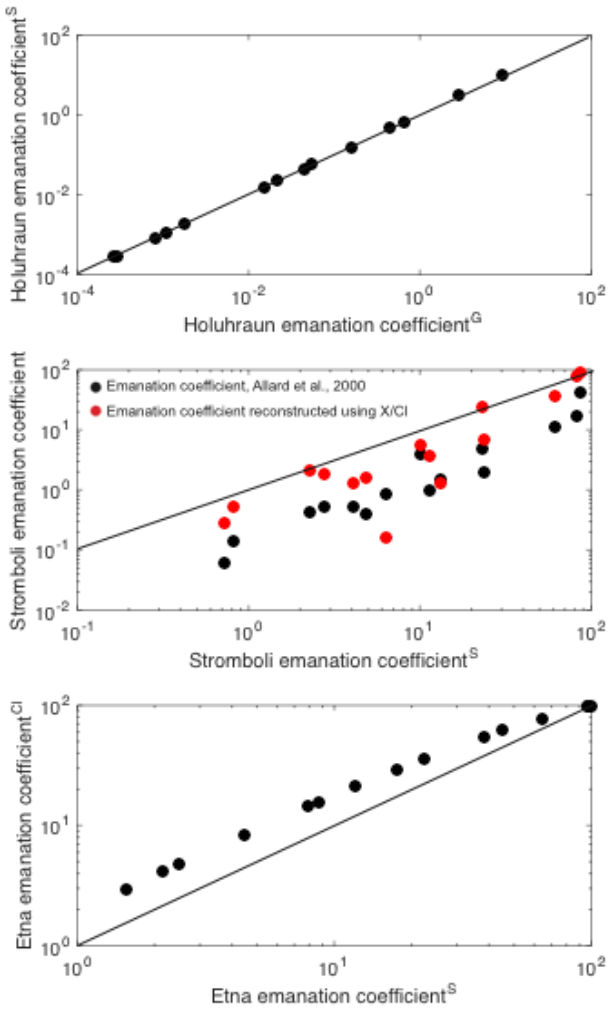

Supplementary Figure 4: top: emanation coefficient for metals and semi-metals from Holuhraun calculated by[6] by using a dilution factor calculated from their measurements of sulfur in vent and plume gases (x axis) versus emanation coefficient calculated in this study using the mass of sulfur outgassed from melt (from melt inclusion and matrix glass microanalysis[28]) and X/SO_2 ratios in the plume) to calculate c_i (y axis). Middle: emanation coefficient for Stromboli metals and semi-metals calculated in this study using X/SO_2 to reconstruct c_i (x axis) plotted versus emanation coefficient from[3] using measurements of the emanation coefficient of ^{210}Pb[23] (black); and using *X/Cl* (this study) to calculate c_i(red) (see table caption and methods for detail). Bottom: comparison between emanation coefficient calculated using X/SO_2 (x axis) with that calculated using *X/Cl* (y axis) to calculate c_i for Mt Etna (Italy). Black solid line is the 1:1 line.

Metal partition coefficients

Table 2: Vapor-melt ($D_{vapor\text{-}melt}$) and sulfide-silicate melt ($D_{sulfide\text{-}silicate\ melt}$) partition coefficients used in this paper. Sources are shown either in column header or in individual cells.

	$D_{vapor\text{-}melt}$ [33]	$D_{vapor\text{-}melt}$	$D_{sulfide\text{-}silicate\ melt}$	$D_{sulfide\text{-}silicate\ melt}$ [34]	$D_{sulfide\text{-}silicate\ melt}$ [35]
U		0.002 to 0.45[36]	0.001[37]		
Cs	2.3 to 5.9	0.5 to 10[38]			
W	1.8 to 4.5	3 to 16[39]		0.003 to 0.1	
Cu	33 to 70	1 to 80[40]	260 to 447[41]	540 to 1040	1042 to 1624
Zn	2.3 to 5	9 to 70	1.9 to 3.1[41]	0.28 to 0.94	2.4 to 4.7
Mo	5.5 to 9.8	9.3 to 523[39]		0.1 to 2.58	
Ag	1.9 to 7	7 to 10[38]	360 to 617[41]	300 to 700	853 to 1528
Sn		0.002 to 0.078[40]		2.4 to 6.0	9 to 13
Sb	0.14 to 2.6	1 to 10[38]	15 to 34[41]	1.4 to 11.2	
As	3 to 6.2	1 to 2.5[42]		0.3 to 19.7	
Pb	8.4 to 15	2 to 14[39]	26 to 54[41]	13 to 48	45 to 71
Tl	3.1 to 6	3.5 to 12.4[39]	10 to 17[41]		
Cd	6.5 to 30		45 to 82[41]		61 to 193
Bi	1 to 5.3	7 to 30[38]		110 to 1130	
Se	0.59 to 12		790 to 1500[41]		
Au		12 to 15[42]		930 to 5500	
Te	0.22 to 6.7		6000 to 16000[41]		

Notes on experimental conditions.

[33] Partitioning of metals between vapor and basalt silicate melt at 850 °C, 2 kbar, Cl- and H_2O-bearing fluids.

[34] Partitioning between basanite melt, sulfide liquid and monosulfide solid solution, at 1175 to 1300 °C, 1.5-3.0 GPa, 3 units below to 1 unit above FMQ buffer, relevant to mantle conditions.

[35] Mid-ocean ridge basalts at FMQ to FMQ-1.

[36] Haplogranite melt composition, aqueous fluid with HCl and HF, 2 kbar, 750 C.

[37] 1-10 GPa, 1750–2100 °C, 0–28 wt% S, and fO_2 2 log units below IW (core conditions).

[38] Granitic and peralkaline melts, melts with high chlorinities (1-14 mole/kg), log fO_2 = NNO−1.7 to NNO+4.5.

[39] Haplogranite melt composition, with H_2O-HCl and H_2O-HF vapor phase. For Cu, lowest $D_{vapor\text{-}melt}$ for H_2O-only and highest for Cl-rich case; for Sn highest $D_{vapor\text{-}melt}$ for Cl-rich case, but poorly constrained.

[40] Haplogranite melt composition, aqueous fluid with HCl and HF, 2 kbar, 750 C.

[41] The silicate constituent was either a MORB or a composition close to the 1.5 GPa eutectic composition in the system anorthite–diopside–forsterite ($An_{50}Di_{28}Fo_{22}$). FeO was added to vary FeO activity.

References

1 Gauthier, P.-J. & Le Cloarec, M.-F. Variability of alkali and heavy metal fluxes released by Mt. Etna volcano, Sicily, between 1991 and 1995. *Journal of Volcanology and Geothermal Research* **81**, 311-326 (1998).

2 Aiuppa, A., Dongarrà, G., Valenza, M., Federico, C. & Pecoraino, G. Degassing of trace volatile metals during the 2001 eruption of Etna. *Volcanism and the Earth's atmosphere*, 41-54 (2003).

3 Allard, P. *et al.* Acid gas and metal emission rates during long- lived basalt degassing at Stromboli volcano. *Geophysical Research Letters* **27**, 1207-1210 (2000).

4 Saunders, J. A. & Brueseke, M. E. Volatility of Se and Te during subduction-related distillation and the geochemistry of epithermal ores of the western United States. *Economic Geology* **107**, 165-172 (2012).

5 Allard, P. *et al.* Prodigious emission rates and magma degassing budget of major, trace and radioactive volatile species from Ambrym basaltic volcano, Vanuatu island Arc. *Journal of Volcanology and Geothermal Research* (2016).

6 Gauthier, P. J., Sigmarsson, O., Gouhier, M., Haddadi, B. & Moune, S. Elevated gas flux and trace metal degassing from the 2014- 2015 fissure eruption at the Bárðarbunga volcanic system, Iceland. *Journal of Geophysical Research: Solid Earth* (2016).

7 Gysi, A. P. & Williams-Jones, A. E. Hydrothermal mobilization of pegmatite-hosted REE and Zr at Strange Lake, Canada: A reaction path model. *Geochimica et Cosmochimica Acta* **122**, 324-352 (2013).

8 Webster, J., Holloway, J. & Hervig, R. Partitioning of lithophile trace elements between H 2 O and H 2 O+ CO 2 fluids and topaz rhyolite melt. *Economic Geology* **84**, 116-134 (1989).

9 Symonds, R. B., Rose, W. I., Reed, M. H., Lichte, F. E. & Finnegan, D. L. Volatilization, transport and sublimation of metallic and non-metallic elements in high temperature gases at Merapi Volcano, Indonesia. *Geochimica et Cosmochimica Acta* **51**, 2083-2101 (1987).

10 Stoiber, R. E. & Rose, W. I. Fumarole incrustations at active Central American volcanoes. *Geochimica et Cosmochimica Acta* **38**, 495-516 (1974).

11 Buat- Ménard, P. & Arnold, M. The heavy metal chemistry of atmospheric rarticulate matter emitted by Mount Etna Volcano. *Geophysical Research Letters* **5**, 245-248 (1978).

12 Mather, T. A. Volcanoes and the environment: Lessons for understanding Earth's past and future from studies of present-day volcanic emissions. *Journal of Volcanology and Geothermal Research* **304**, 160-179 (2015).

13 Mather, T., Pyle, D. & Oppenheimer, C. Tropospheric volcanic aerosol. *Volcanism and the Earth's Atmosphere*, 189-212 (2003).

14 Mather, T. *et al.* Halogens and trace metal emissions from the ongoing 2008 summit eruption of Kīlauea volcano, Hawaii. *Geochimica et Cosmochimica Acta* **83**, 292-323 (2012).

15 Hedenquist, J. W. & Lowenstern, J. B. The role of magmas in the formation of hydrothermal ore deposits. *Nature* **370**, 519-527 (1994).

16 Heinrich, C. A., Ryan, C. G., Mernagh, T. P. & Eadington, P. J. Segregation of ore metals between magmatic brine and vapor; a fluid inclusion study using PIXE microanalysis. *Economic Geology* **87**, 1566-1583 (1992).

17 Zajacz, Z. & Halter, W. Copper transport by high temperature, sulfur-rich magmatic vapor: Evidence from silicate melt and vapor inclusions in a basaltic andesite from the Villarrica volcano (Chile). *Earth and Planetary Science Letters* **282**, 115-121 (2009).

18 Williams, T. J., Candela, P. A. & Piccoli, P. M. The partitioning of copper between silicate melts and two-phase aqueous fluids: an experimental investigation at 1 kbar, 800 C and 0.5 kbar, 850 C. *Contr. Mineral. and Petrol.* **121**, 388-399 (1995).

19 Gladney, E. & Goode, W. Elemental concentrations in eight new United States Geological Survey rock standards: a review. *Geostandards newsletter* **5**, 31-64 (1981).
20 Moune, S., Gauthier, P.-J. & Delmelle, P. Trace elements in the particulate phase of the plume of Masaya Volcano, Nicaragua. *Journal of Volcanology and Geothermal Research* **193**, 232-244 (2010).
21 Mather, T. A. *et al.* Halogens and trace metal emissions from the ongoing 2008 summit eruption of Kīlauea volcano, Hawai`i. *Geochimica et Cosmochimica Acta* **83**, 292-323, doi:http://dx.doi.org/10.1016/j.gca.2011.11.029 (2012).
22 Lambert, G., Le Cloarec, M., Ardouin, B. & Le Roulley, J. Volcanic emission of radionuclides and magma dynamics. *Earth and Planetary Science Letters* **76**, 185-192 (1985).
23 Pennisi, M., Le Cloarec, M., Lambert, G. & Le Roulley, J. Fractionation of metals in volcanic emissions. *Earth and planetary science letters* **88**, 284-288 (1988).
24 Rubin, K. Degassing of metals and metalloids from erupting seamount and mid-ocean ridge volcanoes: Observations and predictions. *Geochimica et Cosmochimica Acta* **61**, 3525-3542 (1997).
25 Sides, I. R., Edmonds, M., Maclennan, J., Swanson, D. A. & Houghton, B. F. Eruption style at Kīlauea Volcano in Hawai`i linked to primary melt composition *Nature Geoscience* **7**, 464–469, doi:doi:10.1038/ngeo2140 (2014).
26 Metrich, N. & Clocchiatti, R. Sulfur abundance and its speciation in oxidized alkaline melts. *Geochimica et Cosmochimica Acta* **60**, 4151-4160 (1996).
27 Bertagnini, A., Métrich, N., Landi, P. & Rosi, M. Stromboli volcano (Aeolian Archipelago, Italy): An open window on the deep- feeding system of a steady state basaltic volcano. *Journal of Geophysical Research: Solid Earth* **108** (2003).
28 Hartley, M. E., Bali, E., Maclennan, J., Neave, D. A. & Halldórsson, S. A. Melt inclusion constraints on petrogenesis of the 2014–2015 Holuhraun eruption, Iceland. *Contr. Mineral. and Petrol.* **173**, 10 (2018).
29 Pennisi, M. & Le Cloarec, M. F. Variations of Cl, F, and S in Mount Etna's plume, Italy, between 1992 and 1995. *Journal of Geophysical Research: Solid Earth* **103**, 5061-5066 (1998).
30 Williams-Jones, G., Rymer, H. & Rothery, D. A. Gravity changes and passive SO2 degassing at the Masaya caldera complex, Nicaragua. *Journal of Volcanology and Geothermal Research* **123**, 137-160 (2003).
31 Edmonds, M., Sides, I. R. & Maclennan, J. Insights into mixing, fractionation and degassing of primitive melts at Kīlauea Volcano, Hawai`i. *AGU Monograph* (2014).
32 Edmonds, M., Gerlach, T. M. & Herd, R. A. Halogen degassing during ascent and eruption of water-poor basaltic magma. *Chemical Geology* **263**, 122-130, doi:http://dx.doi.org/10.1016/j.chemgeo.2008.09.022 (2009).
33 Guo, H. & Audétat, A. Transfer of volatiles and metals from mafic to felsic magmas in composite magma chambers: An experimental study. *Geochimica et Cosmochimica Acta* **198**, 360-378 (2017).
34 Li, Y. & Audétat, A. Partitioning of V, Mn, Co, Ni, Cu, Zn, As, Mo, Ag, Sn, Sb, W, Au, Pb, and Bi between sulfide phases and hydrous basanite melt at upper mantle conditions. *Earth and Planetary Science Letters* **355**, 327-340 (2012).
35 Patten, C., Barnes, S.-J., Mathez, E. A. & Jenner, F. E. Partition coefficients of chalcophile elements between sulfide and silicate melts and the early crystallization history of sulfide liquid: LA-ICP-MS analysis of MORB sulfide droplets. *Chemical Geology* **358**, 170-188 (2013).
36 Keppler, H. & Wyllie, P. J. Role of fluids in transport and fractionation of uranium and thorium in magmatic processes. *Nature* **348**, 531 (1990).

37 Wheeler, K. T., Walker, D., Fei, Y., Minarik, W. G. & McDonough, W. F. Experimental partitioning of uranium between liquid iron sulfide and liquid silicate: Implications for radioactivity in the Earth's core. *Geochimica et Cosmochimica Acta* **70**, 1537-1547 (2006).

38 Zajacz, Z., Halter, W. E., Pettke, T. & Guillong, M. Determination of fluid/melt partition coefficients by LA-ICPMS analysis of co-existing fluid and silicate melt inclusions: controls on element partitioning. *Geochimica et Cosmochimica Acta* **72**, 2169-2197 (2008).

39 MacKenzie, J. M. & Canil, D. Fluid/melt partitioning of Re, Mo, W, Tl and Pb in the system haplobasalt-H 2 O-Cl and the volcanic degassing of trace metals. *Journal of Volcanology and Geothermal Research* **204**, 57-65 (2011).

40 Keppler, H. & Wyllie, P. J. Partitioning of Cu, Sn, Mo, W, U, and Th between melt and aqueous fluid in the systems haplogranite-H2O− HCl and haplogranite-H2O− HF. *Contr. Mineral. and Petrol.* **109**, 139-150 (1991).

41 Kiseeva, E. S. & Wood, B. J. A simple model for chalcophile element partitioning between sulphide and silicate liquids with geochemical applications. *Earth and Planetary Science Letters* **383**, 68-81 (2013).

42 Simon, A. C., Pettke, T., Candela, P. A., Piccoli, P. M. & Heinrich, C. A. The partitioning behavior of As and Au in S-free and S-bearing magmatic assemblages. *Geochimica et Cosmochimica Acta* **71**, 1764-1782 (2007).